On the rigorous justification of b-modulation method and inclusion of discrete eigenvalues

Dmitry Shepelsky, Anastasiia Vasylchenkova, Jaroslaw E. Prilepsky, and Iryna Karpenko

***Abstract*—Addressing the optical communication systems employing the nonlinear Fourier transform (NFT) for the data modulation/demodulation, we provide the explicit proof for the properties of the signals emerging in the so-called b-modulation method, the nonlinear signal modulation technique that provides the explicit control over the signal extent. Our approach ensures that the time-domain profile corresponding to the b-modulated data has a limited duration, including the cases when the bound states (discrete solitonic eigenvalues) are present. In particular, in contrast to the previous approaches, we show that it is possible to include the discrete eigenvalues with the specially chosen parameters into the b-modulation concept while keeping the signal localization property exactly.**

***Index Terms*—Optical fibre communication, optical solitons**

I. Introduction

In a multitude of different physical areas, and, notably, in fibre optics, the signal's evolution can often be well approximated by the nonlinear Schrödinger equation (NLS) [1], [2]. In particular, the latter serves as a leading order model that describes the propagation of light envelope in fibre-optic communication channels under some simplifying conditions [1], [3]. The normalised lossless and noiseless NLS for the slow varying complex electromagnetic field envelope function $q(z,t)$, where z is the distance along the fibre and t is the retarded time (in the fibre optics context), is given as follows

$$iq_z + q_{tt} + 2|q|^2 q = 0\,, \tag{1}$$

i is the imaginary unity; for the explicit normalisations pertaining to single-mode optical fibres, see, e.g., [3]. The important property of NLS (1) is that it belongs to the class of the so-called integrable equations, meaning that the initial-value problem for this equation can be solved by means of inverse scattering technique [2], [4], given some constraints on the "initial conditions", $q(0,t)$ in our notations. The signal processing operations participating in this method are often referred to as the NFT, and the multiplexing technique dealing with the nonlinear Fourier (NF) domain data was coined nonlinear frequency division multiplexing [5]. In a nutshell, the NFT maps the solution of NLS (i.e. our signal) onto the space of the complex-valued spectral parameter k, playing the role of a "nonlinear frequency", such that the NFT operation, Eq. (2) below, decomposes our space-time profile into the nonlinear modes evolving inside the NF domain. The nonlinear spectrum (i.e. the "NFT image") that corresponds to the initial profile with a finite first norm, $q(0,t) \in L^1(\mathbb{R})$, contains, in the general case:

(i) two *scattering coefficients* $a(k)$, $b(k)$ for $k \in \mathbb{R}$ describing the dispersive radiation components of our pulse;
(ii) the discrete (solitonic) spectrum, consisting of two complex parameters for each discrete (soliton) mode: the eigenvalue k_j and the respective spectral amplitude c_j.

Either discrete or continuous part of the NF spectrum can be absent in some specific situations. See more explicit details in [2], [3], [4], [5].

Insofar as the NF modes evolve linearly inside the NF domain, the NFT-based optical signal processing and the usage of the parameters of nonlinear modes as data carriers have been considered as an efficacious method for the nonlinearity mitigation in optical fibre links [3], [5], [6], [7]. The recently introduced b-modulation NFT technique [8], operating with the band-limited $b(k)$ profiles, has been aimed at resolving one of the principal challenges in the NFT-based communication: to

This work was supported in part by the Leverhulm Trust Grant RP-2018-063 and Erasmus+ mobility exchange programme.

D. Shepelsky and I. Karpenko are with B. Verkin Institute for Low Temperature Physics and Engineering, Kharkiv, Ukraine (e-mails: shepelsky@yahoo.com and inic.karpenko@gmail.com).

A. Vasylchenkova and J. E. Prilepsky are with the Aston Instotute of Photonic Technologies, Aston University, Birmingham, B4 7ET, UK (e-mails: vasylcha & y.prylepskiy1@aston.ac.uk).

attain the explicit control over the temporal duration of NFT-generated signals at the transmitter side [9], [10], [11], [12]. The latter property allows us to pack our data better inside a given time-bandwidth volume and, thus, to reach higher spectral efficiency numbers. In particular, the highest data rate reported so far for the NFT-based transmission method was achieved with the modified variant of b-modulation (in the dual-polarisation case) [13] and has very recently been confirmed experimentally [14]. In the case of b-modulation, we map our data on the function $b(k)$, which is chosen to be band-limited, and further adjust the function $a(k)$ accordingly, see the explanations and definitions below in Sec. II. Then, the ensuing signal $q(t)$, obtained through the inverse NFT operation, has a finite duration in time domain [8]. It is exactly the latter feature that allows us to get a higher spectral efficiency compared to "conventional" NFT-based systems employing the continuous NF spectrum modulation [3], [6], see the explicit comparison in [12].

For the completeness of our exposition here, we note that in the original work by Wahls [8], where the b-modulation concept was introduced, the problem of a complete characterization of $b(k)$ in the case of time-limited signals $q(t)$ supporting bound states (i.e. containing a non-zero discrete NF spectrum part) was formulated as an open question. In the follow-up study [12], a necessary condition for the possibility to have bound states keeping the same $b(k)$ was stated and the analogy with the linear operator of the Lax pair representation for the Korteweg–de Vries equation was mentioned. In the latter case we deal with the bound states of one-dimensional Schrödinger equation (written here for some function $\psi(t,k)$),

$$\psi_{tt} + k^2\psi = V(t)\psi.$$

See works [15], [16], where the necessary conditions for $b(k)$ to generate a finitely supported $V(t)$, which serves in this context the role of $q(t)$ from Zakharov-Shabat system (2), are discussed in presence of non-zero discrete spectrum (bound states). We also mention Ref. [17], where the uniqueness of the determination of a time-limited $q(t)$ in (2) from $b(k)$ is discussed in the absence of bound states. At this place we would like to emphasize that the recent work [18] proposes to put an arbitrary additional solitary mode atop the b-modulated profile, but to keep the width of the solitary component in time domain sufficiently thin (actually only one soliton was embedded in that work). Such a composition ensures that the considerable portion of the signal does not spread beyond the initial extent of the b-modulation-generated profile. Importantly, this approach *does not provide the truly localised signals*, and in our current study we require the strict localisation of the time-domain signal, similarly to the initial definition of b-modulation [8].

In this paper, we analyse the b-modulated signals making an emphasis on the sufficiency aspect. Namely, applying the Riemann–Hilbert approach [5], [19], [20] for solving the inverse scattering problem for Zakharov-Shabat system (2), we *characterize* the time-limited signals having the same scattering coefficient $b(k)$ showing, in particular, that it is possible to include the discrete nonlinear spectral components (solitons) into the b-modulation without violating the complete localisation of respective time-domain profile.

II. Derivation of the properties for b-modulated signals

A. Direct problem for the Zakharov-Shabat system attributed to $q(t)$ with a finite extent.

The forward NFT for the signals $q(t,z)$ evolving according to Eq. (1), is performed by considering the Zakharov-Shabat system for two-component function $\varphi(t,k)$ [4], where here and in the following we drop the dependencies of all quantities on z for simplicity:

$$\varphi_t + ik\sigma_3\varphi = Q(t)\varphi, \qquad Q(t) = \begin{pmatrix} 0 & q(t) \\ -\bar{q}(t) & 0 \end{pmatrix}. \tag{2}$$

Here and in the sequel the overbar means the complex conjugate, and $\sigma_3 = \left(\begin{smallmatrix} 1 & 0 \\ 0 & -1 \end{smallmatrix}\right)$. We assume that for $t \in \mathbb{R}$, $q \in L^1(\mathbb{R})$ and $q(t) = 0$ for $|t| > \frac{L}{2}$ for some positive quantity $L > 0$, which is our localisation extent.

Let us define the two-component Jost solutions $\Phi^{(j)}(t,k)$ and $\Psi^{(j)}(t,k)$, $j = 1, 2$, of Eq. (2), for $k \in \mathbb{R}$, fixed by their asymptotic behaviour:

$$\Phi^{(1)}(t,k) \equiv [\phi_1, \phi_2]^T \to [e^{-ikt}, 0]^T \quad \text{as } t \to -\infty,$$

$$\Psi^{(2)}(t,k) \equiv [\psi_1, \psi_2]^T \to [0, e^{ikt}]^T \quad \text{as } t \to \infty,$$

and $\Phi^{(2)} = [-\bar{\phi}_2, \bar{\phi}_1]^T$, $\Psi^{(1)} = [\bar{\psi}_2, -\bar{\psi}_1]^T$. The scattering coefficients $a(k)$ and $b(k)$ associated with

a given $q(t)$, are defined through the scattering relation:

$$\Phi(t,k) = \Psi(t,k) \begin{pmatrix} a(k) & -\bar{b}(k) \\ b(k) & \bar{a}(k) \end{pmatrix}, \quad k \in \mathbb{R}, \quad (3)$$

with

$$|a(k)|^2 + |b(k)|^2 \equiv 1.$$

In Eq. (3) $\Phi = (\Phi^{(1)}, \Phi^{(2)})$, and similarly for Ψ. Now notice that for finite-extent $q(t)$, $\Phi(t,k)$ and $\Psi(t,k)$ are the entire analytic functions of $k \in \mathbb{C}$. Moreover, in this case (3) holds for all $k \in \mathbb{C}$ with $\bar{a}$, $\bar{b}$ replaced by a^*, b^*, where the asterisk means the Schwarz reflection: $\varphi^*(k) := \overline{\varphi(\bar{k})}$. Consequently,

$$a^*(k)a(k) + b^*(k)b(k) \equiv 1, \quad k \in \mathbb{C}. \quad (4)$$

It is well-known that if $q(t) = 0$ for $|t| > \frac{L}{2}$ with some $L > 0$, then the associated spectral functions $a(k)$ and $b(k)$ can be expressed via the Fourier transforms of some finitely supported functions. For the consistency of presentation, we give here a simple proof of this property using the integral representations for the Jost solutions (cf. [17]).

Theorem 2.1: Let $q \in L^1(\mathbb{R})$ be such that $q(t) = 0$ for $|t| > \frac{L}{2}$ for some $L > 0$. Then

- $\Phi(t,k) = e^{-ikt\sigma_3}$ for $t < -\frac{L}{2}$, and

$$\Phi(t,k) = e^{-ikt\sigma_3} + \int_{-L-t}^{t} K_1(t,\tau) e^{-ik\tau\sigma_3} d\tau, \quad t > -\frac{L}{2}; \quad (5)$$

- $\Psi(x,k) = e^{-ikt\sigma_3}$ for $t > \frac{L}{2}$, and

$$\Psi(t,k) = e^{-ikt\sigma_3} + \int_{t}^{L-t} K_2(t,\tau) e^{-ik\tau\sigma_3} d\tau, \quad t < \frac{L}{2}. \quad (6)$$

Here $K_j(t,\cdot) \in L^1$, $j = 1, 2$, are some 2×2 matrix functions.

Proof of Theorem 2.1: For any $q(t) \in L^1(\mathbb{R})$, the integral representation for Φ has the form [4]:

$$\Phi(t,k) = e^{-ikt\sigma_3} + \int_{-\infty}^{t} K_1(t,\tau) e^{-ik\tau\sigma_3} d\tau. \quad (7)$$

Assuming for a moment that $q(t)$ is smooth ($q(t) \in C^1(\mathbb{R})$) and substituting (7) into (2), it follows that $K_1(t,\tau)$ satisfies the system of equations:

$$\begin{aligned} &K_1(t,t) - \sigma_3 K_1(t,t)\sigma_3 = Q(t), \\ &K_{1t}(t,\tau) + \sigma_3 K_{1\tau}(t,\tau)\sigma_3 - Q(t)K_1(t,\tau) = 0, \quad \tau < t, \end{aligned} \quad (8)$$

where $Q(t)$ is given in Eq. (2). Decomposing K_1 into the diagonal and off-diagonal parts, K_1^d and K_1^o, respectively,

$$K_1 = K_1^o + K_1^d,$$

Eq. (8) then reduces to

$$\begin{aligned} &K_1^o(t,t) = \frac{1}{2} Q(t), \\ &K_{1t}^o(t,\tau) - K_{1\tau}^o(t,\tau) - Q(t)K_1^d(t,\tau) = 0, \quad \tau < t, \\ &K_{1t}^d(t,\tau) + K_{1\tau}^d(t,\tau) - Q(t)K_1^o(t,\tau) = 0, \quad \tau < t. \end{aligned} \quad (9)$$

Now changing the variables as $\xi = t + \tau$, $\eta = t - \tau$, and $\tilde{K}(\xi,\eta) := K_1(t,\tau)$, with $\tilde{K}_\xi = \frac{1}{2}(K_{1t} + K_{1\tau})$, $\tilde{K}_\eta = \frac{1}{2}(K_{1t} - K_{1\tau})$, system (9) reduces to the following one:

$$\begin{aligned} &\tilde{K}^o(\xi,0) = \frac{1}{2} Q\left(\frac{\xi}{2}\right), \\ &\tilde{K}_\eta^o(\xi,\eta) = \frac{1}{2} Q\left(\frac{\xi+\eta}{2}\right) \tilde{K}^d(\xi,\eta), \quad \eta > 0, \\ &\tilde{K}_\xi^d(\xi,\eta) = \frac{1}{2} Q\left(\frac{\xi+\eta}{2}\right) \tilde{K}^o(\xi,\eta), \quad \eta > 0. \end{aligned} \quad (10)$$

In turn, Eq. (10) reduces to an integral equation of Volterra type. Indeed, integrating (10) we have:

$$\begin{aligned} \tilde{K}^o(\xi,\eta) &= \tilde{K}^o(\xi,0) + \frac{1}{2}\int_0^\eta Q\left(\frac{\xi+\eta'}{2}\right) \tilde{K}^d(\xi,\eta') d\eta' \\ &= \frac{1}{2} Q\left(\frac{\xi}{2}\right) + \frac{1}{2}\int_0^\eta Q\left(\frac{\xi+\eta'}{2}\right) \tilde{K}^d(\xi,\eta') d\eta', \\ \tilde{K}^d(\xi,\eta) &= \frac{1}{2}\int_{-\infty}^{\xi} Q\left(\frac{\xi'+\eta}{2}\right) \tilde{K}^o(\xi',\eta) d\xi'. \end{aligned} \quad (11)$$

Substituting the second expression from Eq. (11) into the first one, we arrive at a single integral equation:

$$\begin{aligned} \tilde{K}^o(\xi,\eta) = \frac{1}{2} Q\left(\frac{\xi}{2}\right) + \frac{1}{4}\int_0^\eta Q\left(\frac{\xi+\eta'}{2}\right) \times \\ \times \int_{-\infty}^{\xi} Q\left(\frac{\xi'+\eta'}{2}\right) \tilde{K}^o(\xi',\eta')\, d\xi'\, d\eta'. \end{aligned} \quad (12)$$

Now notice that for $\xi < -L$, we have $Q\left(\frac{\xi}{2}\right) = 0$, and, thus, Eq. (12) becomes a homogeneous Volterra integral equation (in the domain $\xi < -L$, $\eta > 0$), the unique solution of which is 0. Therefore, $\tilde{K}(\xi,\eta) \equiv 0$ for $\xi < -L$, $\eta > 0$, and, thus, $K_1(t,\tau) = 0$ for $t + \tau < -L$. The general case of $q \in L^1$ follows further by approximating Q in (12) by smooth functions.

Similarly, $\Psi(t,k)$ has the representation

$$\Psi(t,k) = e^{-ikt\sigma_3} + \int_t^\infty K_2(t,\tau)e^{-ik\tau\sigma_3}d\tau,$$

where, actually, $K_2(t,\tau) = 0$ for $t+\tau > L$, which can be proven by following the similar arguments as above and taking into account that $Q(\xi/2) = 0$ for $\xi > L$. ■

Corollary 2.2: 1) In this case, the associated scattering functions $a(k)$ and $b(k)$ have the following integral representations:

$$a(k) = 1 + \int_0^{2L} \alpha(\tau)e^{ik\tau}d\tau, \quad b(k) = \int_{-L}^{L} \beta(\tau)e^{ik\tau}d\tau, \tag{13}$$

with some $\alpha(\tau) \in L^1(0,2L)$, $\beta(\tau) \in L^1(-L,L)$.

2) For $t > L/2$, $b(k)e^{2ikt} \to 0$ as $k \to \infty$ for $k \in \mathbb{C}_+$, and $b^*(k)e^{-2ikt} \to 0$ as $k \to \infty$ for $k \in \mathbb{C}_-$.

Here and below, $\mathbb{C}_\pm = \{k \in \mathbb{C} : \pm\Im k > 0\}$.

3) For $t < -L/2$, $b^*(k)e^{-2ikt} \to 0$ as $k \to \infty$ for $k \in \mathbb{C}_+$, and $b(k)e^{2ikt} \to 0$ as $k \to \infty$ for $k \in \mathbb{C}_-$.

Indeed, setting $t = -L/2$ in the scattering relation (3), and using Eq. (6) and the fact that $\Phi(-\frac{L}{2},k) = e^{ik\frac{L}{2}\sigma_3}$, it follows that a and b have the representations in form of Eq. (13), where $\alpha(\tau) = (K_2)_{22}\left(-\frac{L}{2}, \tau - \frac{L}{2}\right)$ and $\beta(\tau) = -(K_2)_{21}\left(-\frac{L}{2}, \frac{L}{2} - \tau\right)$. Here the double subscript $(\cdot)_{ij}$ stands for the corresponding matrix entry. Items 2) and 3) directly follow from Eq. (13).

B. Inverse problem attributed to band-limited $b(k)$.

In the general case $q(t) \in L^1(\mathbb{R})$, we have [2]: $a(k) = 1 + \int_0^\infty \alpha(\tau)e^{ik\tau}d\tau$ and $b(k) = \int_{-\infty}^\infty \beta(\tau)e^{ik\tau}d\tau$ with $\alpha(\tau) \in L^1(0,\infty)$ and $\beta(\tau) \in L^1(-\infty,\infty)$, and the set of spectral data determining uniquely $q(t)$, is conventionally characterised assuming that $a(k) \neq 0$ for $k \in \mathbb{R}$ and all zeros of $a(k)$ in $\mathbb{C}_+$ are simple; consequently, the number of these zeros is finite, and $|b(k)| < 1$ for all $k \in \mathbb{R}$. With this assumption, the characteristic spectral data consist of $b(k)$, $k \in \mathbb{R}$ and the discrete set $\{k_j, c_j\}_1^N$ (possibly empty), where k_j with $\Im k_j > 0$, $j = 1,\dots,N$, are the zeros of $a(k)$, and $\{c_j\}_1^N$ are the associated norming constants. Moreover, the inverse mapping can be described as follows [2]:

1) Given $b(k)$ and $\{k_j\}_1^N$, construct $a(k)$ in accordance with (4) for $k \in \mathbb{R}$:

$$a(k) = \prod_{j=1}^N \frac{k-k_j}{k-\bar{k}_j} \exp\left\{\frac{1}{2\pi i}\int_{\mathbb{R}} \frac{\log(1-|b(s)|^2)}{s-k}ds\right\}; \tag{14}$$

2) Define the reflection coefficient

$$r(k) := b(k)/a(k), \qquad k \in \mathbb{R}; \tag{15}$$

3) Solve the Riemann–Hilbert problem (RHP): find a 2×2 function $M(t,k)$ satisfying the following conditions:
   - As a function of k, M is meromorphic in $\mathbb{C}\setminus\mathbb{R}$.
   - The limiting values $M_\pm(t,k)$, $k \in \mathbb{R}$ of $M(t,k)$ as k approaches the real line from $\mathbb{C}_\pm$ are related by
   $$M_+(t,k) = M_-(t,k)J(t,k), \qquad k \in \mathbb{R}, \tag{16}$$
   where
   $$J(t,k) = \begin{pmatrix} 1+|r(k)|^2 & r^*(k)e^{-2ikt} \\ r(k)e^{2ikt} & 1 \end{pmatrix}. \tag{17}$$
   - $M(t,k) \to I$ as $k \to \infty$.
   - The singularities of M are characterised as follows: $M^{(1)}(t,k)$ has simple poles at $\{k_j\}_1^N$ and $M^{(2)}(t,k)$ has simple poles at $\{\bar{k}_j\}_1^N$ such that the following residue conditions hold:
   $$\operatorname{Res} M^{(1)}(t,k)\Big|_{k=k_j} = c_j e^{2ik_jt}M^{(2)}(t,k_j), \tag{18}$$
   $$\operatorname{Res} M^{(2)}(t,k)\Big|_{k=\bar{k}_j} = -\bar{c}_j e^{-2i\bar{k}_jt}M^{(1)}(t,\bar{k}_j). \tag{19}$$

4) Having the RHP solved, $q(t)$ can be obtained by
$$q(t) = 2iM^1_{12}(t),$$
where $M^1(t)$ emerges from the large-k asymptotic of $M(t,k)$:
$$M(t,k) = I + \frac{M^1(t)}{k} + O(k^{-2}), \qquad k \to \infty.$$

Our main result consists in the characterisation of the spectral data in the case of finitely supported $q(t)$, and is given in the following theorem.

Theorem 2.3: Let $b(k)$ be given such that

(i) $b(k) = \int_{-L}^{L} \beta(\tau)e^{ik\tau}d\tau$ with some $\beta(\tau) \in L^1(-L,L)$, and

(ii) the function $G(k) := 1 - b^*(k)b(k)$ has no zeros for $k \in \mathbb{R}$ (or, equivalently, $G(k) > 0$ for $k \in \mathbb{R}$).

Denote by $\mathcal{A}_b$ the set of all zeros of $G(k)$. Then:

1) The set $\mathcal{F}_b$ of all $q \in L^1$ such that $b(k)$ is the spectral function associated to q by the direct mapping, is infinite;
2) $q(t) = 0$ for $|t| > L/2$, for any $q \in \mathcal{F}_b$.
3) Given $b(k)$, each $q \in \mathcal{F}_b$ is characterized by a finite subset of $\mathcal{A}_b \cap \mathbb{C}_+$. The latter constitutes the set of simple zeros of the spectral function $a(k)$ associated to this q.

Remark 2.4: $M(t,k)$ is related to the Jost solutions of Zakharov-Shabat problem (2) as follows

$$M(t,k) = \begin{cases} \left(\frac{\Phi^{(1)}(t,k)}{a(k)}, \Psi^{(2)}(t,k)\right) e^{ikt\sigma_3}, & k \in \mathbb{C}_+, \\ \left(\Psi^{(1)}(t,k), \frac{\Phi^{(2)}(t,k)}{a^*(k)}\right) e^{ikt\sigma_3}, & k \in \mathbb{C}_-. \end{cases}$$

Proof of Theorem 2.3. The proof is based on using the flexibility of RHP formalism: (i) the same $q(t)$ can be retrieved from the solutions of different RHPs; (ii) we can proceed from one RHP to another (that produces the same $q(t)$) by appropriately "deforming" the original RHP, i.e. deforming the jump contour and the associated jump matrices entering the definition of RHP.

First, notice that in our case $b(k)$ is analytic in $\mathbb{C}$ and, thus, the norming constants are determined by $b(k)$ and $a(k)$:

$$c_j = \frac{b(k_j)}{\dot{a}(k_j)}, \tag{20}$$

where the overdot means the derivative with respect to k. Also, $G(k)$, as well as $b(k)$, is an entire function of exponential type. It follows from the Hadamard factorisation theorem [21] combined, e.g., with the evaluation of $G(k)$ for large real k, that the number of zeros of $G(k)$ is infinite. In turn, it follows from (4) that the set $\mathcal{A}_b$ (determined by $b(k)$ and symmetric w.r.t. the real axis) is a union of zeros of $a(k)$ and $a^*(k)$. Consequently, all zeros of $a(k)$ in $\mathbb{C}_+$ (the eigenvalues of (2)) must be contained in $\mathcal{A}_b \cap \mathbb{C}_+$.

Let us choose any finite (particularly, it can be empty) subset $\{k_j\}_1^N$ from $\mathcal{A}_b \cap \mathbb{C}_+$ and construct $a(k)$ according to (14). Our main point is that using $b(k)$, $a(k)$, and $\{k_j, c_j\}_1^N$, specified above, as the spectral data and the input to RHP, Eqs. (16)–(19), one always arrives at such $q(t)$ that $q(t) = 0$ for $|t| > L/2$.

Proof that $q(t) = 0$ for $t > L/2$: The proof is based on the deformation of RHP (16)–(19) suggested by the following algebraic factorization of J in (17):

$$J(t,k) = \begin{pmatrix} 1 & r^*(k)e^{-2ikt} \\ 0 & 1 \end{pmatrix} \begin{pmatrix} 1 & 0 \\ r(k)e^{2ikt} & 1 \end{pmatrix}, \qquad k \in \mathbb{R}.$$

Introduce

$$\hat{M}(t,k) := \begin{cases} M(t,k) \begin{pmatrix} 1 & 0 \\ -r(k)e^{2ikt} & 1 \end{pmatrix}, & k \in \mathbb{C}_+, \\ M(t,k) \begin{pmatrix} 1 & r^*(k)e^{-2ikt} \\ 0 & 1 \end{pmatrix}, & k \in \mathbb{C}_-. \end{cases} \tag{21}$$

Notice that the triangular matrix factors in (21) are such that (i) they are meromorphic in the respective half-planes and (ii) they approach I as $k \to \infty$. The latter follows from Corollary 2.2, item 2, and the fact that $a(k) \to 1$ as $k \to \infty$ for $k \in \mathbb{C}_+$. Moreover, the off-diagonal entries of these factors decay to 0 exponentially fast for each fixed $t > L/2$. The latter means that for the large-k asymptotics of $\hat{M}(t,k)$, we have $\hat{M}^1_{12}(t) = M^1_{12}(t)$ for $t > L/2$. Consequently, for $\hat{q}(t)$ obtained from the large-k asymptotics of $\hat{M}(t,k)$, we have:

$$\hat{q}(t) = q(t), \quad t > L/2. \tag{22}$$

On the other hand, $\hat{M}(t,k)$ can be characterized as the solution of the RHP with the trivial jump conditions: $\hat{M}(t,k)$ is analytic $\mathbb{C} \setminus \mathbb{R}$ such that

$$\begin{aligned} \hat{M}_+(t,k) &= \hat{M}_-(t,k), \qquad k \in \mathbb{R}, \\ \hat{M}(t,k) &\to I, \qquad k \to \infty. \end{aligned} \tag{23}$$

Indeed, this is obvious in the case when $a(k)$ has no zeros in $\mathbb{C}_+$. If $a(k_j) = 0$ for some $k_j \in \mathbb{C}_+$, we evaluate $\hat{M}^{(1)}(t,k)$ as $k \to k_j$ by using

$$\hat{M}^{(1)}(t,k) = M^{(1)}(t,k) - \frac{b(k)}{a(k)} e^{2ikt} M^{(2)}(t,k)$$

that follows from Eq. (21). Taking into account (18), it then follows that, as $k \to k_j$,

$$\begin{aligned} \hat{M}^{(1)}(t,k) &= \frac{1}{k-k_j} \frac{b(k_j)}{\dot{a}(k_j)} e^{2ik_jt} M^{(2)}(t,k_j) + O(1) \\ &- \left(\frac{b(k_j)}{\dot{a}(k_j)(k-k_j)} e^{2ik_jt} M^{(2)}(t,k_j) + O(1) \right) = O(1). \end{aligned}$$

Therefore, $\hat{M}^{(1)}(t,k)$ has no singularity at $k = k_j$. Similarly for $\hat{M}^{(2)}(t,k)$ at $k = \bar{k}_j$.

Since the (unique) solution of RHP (23) is the trivial one: $\hat{M}(t,k) \equiv I$ for all t, it follows that $\hat{M}^1_{12}(t) = 0$. Consequently, $\hat{q}(t) \equiv 0$ and thus, in view of Eq. (22), $q(t) = 0$ for $t > L/2$. ■

Proof that $q(t) = 0$ for $t < -L/2$: Like above, the proof is based on the deformations of the (original) RHP, Eqs. (16)–(19). But now it is convenient to split the appropriate deformation into two steps.

Step 1. Define

$$\tilde{M}(t,k) := \begin{cases} M(t,k)\begin{pmatrix} a(k) & 0 \\ 0 & \frac{1}{a(k)} \end{pmatrix}, & k \in \mathbb{C}_+, \\ M(t,k)\begin{pmatrix} \frac{1}{a^*(k)} & 0 \\ 0 & a^*(k) \end{pmatrix}, & k \in \mathbb{C}_-. \end{cases} \tag{24}$$

Then, it follows from Eqs. (16) and (17) that $\tilde{M}(t,k)$ satisfies the following jump conditions for $k \in \mathbb{R}$: $\tilde{M}_+(t,k) = \tilde{M}_-(t,k)\tilde{J}(t,k)$, where

$$\begin{aligned} \tilde{J}(t,k) &= \begin{pmatrix} a^*(k) & 0 \\ 0 & \frac{1}{a^*(k)} \end{pmatrix} \begin{pmatrix} 1+|r(k)|^2 & r^*(k)e^{-2ikt} \\ r(k)e^{2ikt} & 1 \end{pmatrix} \\ &\times \begin{pmatrix} a(k) & 0 \\ 0 & \frac{1}{a(k)} \end{pmatrix} \\ &= \begin{pmatrix} 1 & 0 \\ \frac{b(k)}{a^*(k)}e^{2ikt} & 1 \end{pmatrix} \begin{pmatrix} 1 & \frac{b^*(k)}{a(k)}e^{-2ikt} \\ 0 & 1 \end{pmatrix}. \end{aligned} \tag{25}$$

Step 2. The triangular factorization in (25) suggests introducing the second RHP deformation step, defining $\check{M}$ by

$$\check{M}(t,k) := \begin{cases} \tilde{M}(t,k)\begin{pmatrix} 1 & -\frac{b^*(k)}{a(k)}e^{-2ikt} \\ 0 & 1 \end{pmatrix}, & k \in \mathbb{C}_+, \\ \tilde{M}(t,k)\begin{pmatrix} 1 & 0 \\ \frac{b(k)}{a^*(k)}e^{2ikt} & 1 \end{pmatrix}, & k \in \mathbb{C}_-. \end{cases} \tag{26}$$

Now notice that the triangular factors in (26) are again meromorphic in the respective half-planes and, in view of Corollary 2.2, item 3, they approach I as $k \to \infty$, if $t < -L/2$. Consequently, for $\check{q}(t)$ obtained from the large-k asymptotics of $\check{M}(t,k)$ we have:

$$\check{q}(t) = q(t), \quad t < -L/2. \tag{27}$$

On the other hand, by using the reasoning as in the case $t > L/2$, we can show that $\check{M}(t,k)$ has no singularities in $\mathbb{C} \setminus \mathbb{R}$ and, thus, $\check{M}(t,k)$ can be characterised as the solution of the (piecewise analytic) RHP with the trivial jump conditions, which implies that $\check{M}(t,k) \equiv I$ and thus $\check{q}(t) \equiv 0$. In view of Eq. (27), $q(t) = 0$ for $t < -L/2$, which completes the proof of Theorem 2.3. ■

III. Generation of localised b-modulated profiles containing solitons

According to the discussion above, in order to embed the discrete spectrum components to the signal generated via the b-modulation, which would not destroy the localisation of the signal in time domain, the embedded discrete eigenvalues, $k_{\text{eig}} \in \{k_j\}_1^N$, must satisfy the condition, following from Eq. (4) and item 3 of Theorem 2.3:

$$b^*(k_{\text{eig}})b(k_{\text{eig}}) = 1. \tag{28}$$

For the known analytical expression for $b(k)$, as it occurs in the optical transmission tasks employing b-modulation, we can numerically seek for such points in the upper complex half-plane of parameter k. Then, this points give us the location where we can place our solitary modes without destroying the complete localisation of the time domain signal.

In the b-modulation approach, the signal power is manipulated by scaling of the modulated waveforms. However, this adjustment is typically performed numerically because of the non-trivial dependency between $b(k)$ and $q(t)$ scalings. In particular, let $b(k) = Au(k)$, where $u(k)$ is the waveform modulated in a known way independently of desired signal power, and assume that we do not have discrete spectrum. The signal energy, given by the expression through the nonlinear spectrum functions as [12]

$$\epsilon = -1/\pi \int_{-\infty}^{\infty} \log\left(1 - A^2|u(k)|^2\right) dk,$$

together with the desired time support value L, define the average signal power $P = \epsilon/L$ (in normalised units). Thus, having defined the particular signal power and modulation type, we can calculate the scaling factor A and, therefore, further define the locus of "allowed" eigenvalues, i.e. the eigenvalues that would not destroy the exact localisation, exploiting the theoretical results from Sec. II.

Here we present the procedure of generation of the b-modulated signal with discrete NF eigenmodes, which conserves the signal localisation, employing two simple carrier waveforms that are

commonly used within b-modulation approach [8], [12]: the Nyquist shape, i.e. the sinc function in k-domain and rectangular profile in the corresponding Fourier-conjugated domain, and the flat-top window carrier function, introduced in [12] as a way of overcoming the b-modulated signal power constraint. The studied waveforms used for the $b(k)$ modulation with their corresponding Fourier images are given in Fig. 1.

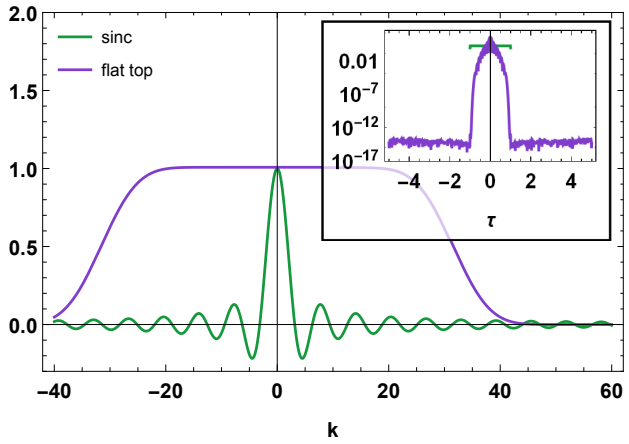

Fig. 1: The waveforms used in our work as an example for the illustration of b-modulation method with their Fourier transforms in the inset.

Depending on the value of scaling factor A, these functions have the points in the complex plane of k, which can be used to implant our eigenvalues at, while keeping the exact localisation of the resulting $q(t)$ profile. Of course, the numerical search cannot guarantee that we have identified all appropriate points, but at the moment we just need to find some of them to illustrate the idea. Typically, for the communication purposes we do not use the eigenvalues with large real and/or imaginary parts. This occurs in view of the numerical issues associated with the inverse NFT computation for high-amplitude solitons, or since, e.g., the nonlinear eigenmode with the large real part of its k_{eig} would rapidly escape from the dedicated time-window during the signal propagation. The numerically found set of points, which can be used as an eigenvalue locus for our studied $b(k)$ waveforms and different scaling factors, are given in Fig. 2. Note that according to Theorem 2.3 for any band-limited $b(k)$ we always have an infinite number of such points.

The procedure of adding the eigenmodes to the b-modulated signal while keeping its exact localisation that can be used in optical communications to

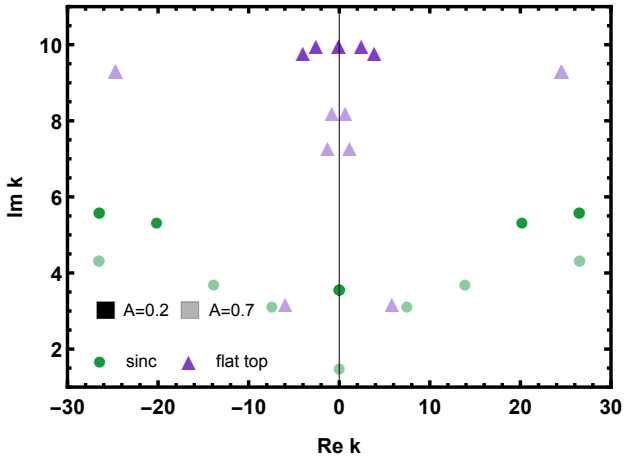

Fig. 2: The points in the complex k-plane, available for out placing the eigenvalues at, when keeping the exact localisation. These soliton modes atop the continuous b-modulated NF spectrum can be used as additional degrees of freedom bearing encoded data in b-modulated signal. The transparency scale is used for different A values. As we see, the points depend on the scaling parameter A used for signal power manipulation.

improve the effectiveness of b-modulation method, is the following.

(i) Modulate the waveform $u(k)$ with the given information and according to desired temporal support L of the signal.
(ii) Choose the desired signal power (without eigenvalues, as in [12]) and find the appropriate scaling factor A. Further define the b-function as $b(k) = Au(k)$.
(iii) For this $b(k)$, find point(s) $k_{\text{eig}} \in \mathbb{C}_+$, which satisfy $b^*(k_{\text{eig}})b(k_{\text{eig}}) = 1$.
(iv) Derive corresponding $a(k)$ via Eq. (14), and calculate the resulting $r(k)$ via Eq. (15);
(v) For each eigenvalue, calculate corresponding $b_{\text{eig}} := b(k_{\text{eig}})$, which uniquely defines the respective norming constant c_{eig} via Eq. (20).
(vi) Generate the signal from the scattering data $r(k)$ and set of $\{k_{\text{eig}}, c_{\text{eig}}\}$ via any inverse NFT procedure[3], e.g. through the Darboux transform [7] or by solving the inverse problem directly with the account of discrete modes.

We perform the numerical mapping to the time domain from the scattering data using the layer-peeling algorithm (in particular, its fast implementation [22], [23]) with the subsequent Darboux transform [7], [24] that adds discrete nonlinear modes to the

continuous ones without affecting the latter. The whole procedure follows the scheme given above. The results of the signal generation for both initial waveforms used for b-modulation and different scaling factor A values are given in Figs. 3–4.

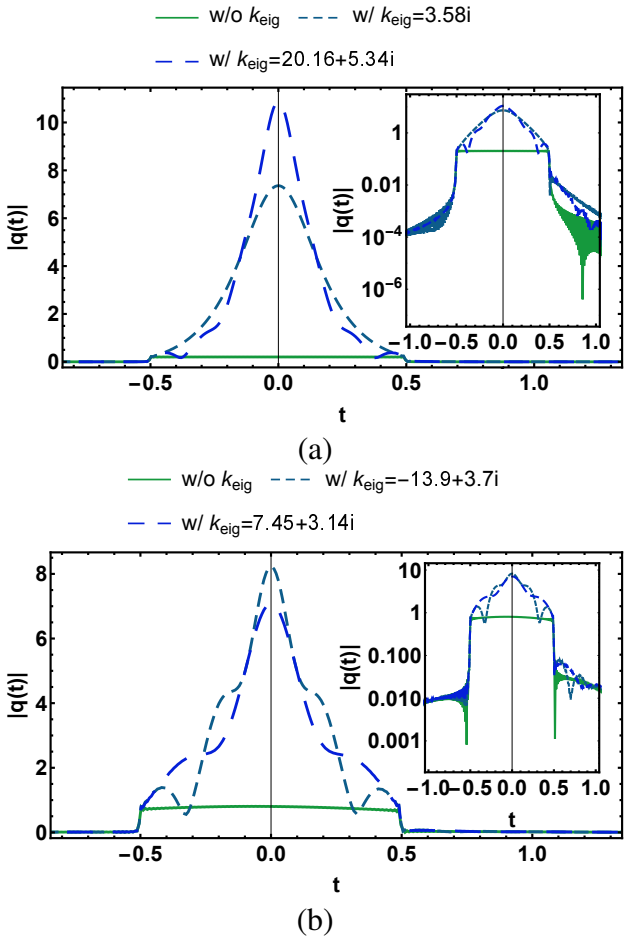

Fig. 3: The signals, generated from the Nyquist waveform via INFT with (dashed) and without (solid) additional eigenvalues embedded, for scaling factors (a) $A = 0.2$ and (b) $A = 0.7$, and different eigenvalues k_{eig}, marked in the figure.

We observe that the signals with additional solitonic eigenvalues have at least not worth localisation than the initial b-modulated signal without discrete eigenmodes, in accordance to our theory. However, the numerical algorithms introduce the additional error, which somewhat deteriorates the expected perfect localisation of the resulting $q(t)$ profile. It can be better seen from the logarithmically scaled plots, given at the insets, that the signal tails decay rates for the profiles with and without additional discrete eigenmodes coincide almost exactly. In spite of the observed insignificant numerical errors, the results

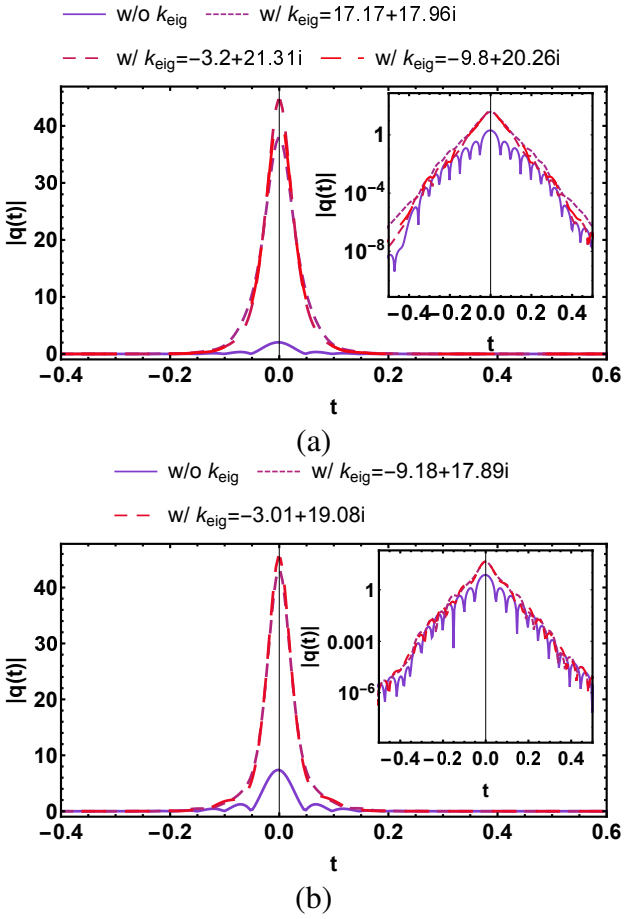

Fig. 4: The signals, generated from the flat-top waveform via INFT with (dashed) and without (solid) additional eigenvalues embedded, for scaling factors (a) $A = 0.2$ and (b) $A = 0.7$, and different eigenvalues k_{eig}, marked in the figure.

in Figs. 3–4 evidently confirm the correctness of the analytical statements presented in our work.

IV. Conclusion

In this work, we filled the gap in the rigorous mathematical formulation of the b-modulation method, constituting the most efficient up to date technique within the NFT-based communications. We presented the explicit proofs providing the one-to-one correspondence between the nonlinear spectrum, which satisfies the requirements of b-modulation, and the optical signal with finite predefined time support. In addition, we presented the full procedure and the mathematical proofs related to uttely important open question: how to implant the discrete solitary modes into the b-modulation concept without violating the condition of the exact localisation of the time-domain profile. Our results

were eventually illustrated and satisfactory validated through the direct numerical analysis. The additional solitonic modes can be used to reach higher signal powers providing, as a result, the better performance and flexibility for b-modulated long-haul optical transmission systems. There also emerges an interesting question of whether the solitonic modes embedded in b-modulation can be used as additional data carriers.

REFERENCES

[1] G. P. Agrawal *Fiber-Optic Communication Systems*, 4th ed., Wiley-Blackwell, 2010.

[2] L. D. Faddeev and L. Takhtajan, *Hamiltonian Methods in the Theory of Solitons*, Springer, 2007.

[3] S. K. Turitsyn, J. E. Prilepsky, S. T. Le, S. Wahls, L. L. Frumin, M. Kamalian, and S. A. Derevyanko, "Nonlinear Fourier transform for optical data processing and transmission: advances and perspectives," *Optica*, vol. 4, pp. 307–322, 2017.

[4] V. E. Zakharov and A. B. Shabat, "Exact theory of 2-dimensional self-focusing and one-dimensional self-modulation of waves in nonlinear media," *Sov. Phys.-JETP*, vol. 34, pp. 62–69, 1972.

[5] M. I. Yousefi and F. R. Kschischang, "Information Transmission Using the Nonlinear Fourier Transform, Parts I – III," *IEEE Trans. Inf. Theory*, vol. 60, pp. 4312–4369, 2014.

[6] S. T. Le, J. E. Prilepsky, and S. K. Turitsyn, "Nonlinear inverse synthesis for high spectral efficiency transmission in optical fibers." *Optics Express*, vol. 22, pp. 26720–26741, 2014.

[7] S. T. Le, V. Aref, and H. Bülow, "Nonlinear signal multiplexing for communication beyond the Kerr nonlinearity limit." *Nat. Photon.*, vol. 11, no. 9, pp. 570–577, 2017.

[8] S. Wahls, "Generation of Time-Limited Signals in the Nonlinear Fourier Domain via b-Modulation," in *Proc. 2017 European Conference on Optical Communication (ECOC)*, Sweden, 2017.

[9] S. T. Le, K. Schuh, F. Buchali, and H. Bülow, "100 Gbps b-modulated Nonlinear Frequency Division Multiplexed Transmission," in *Proc. Optical Fiber Communication Conference (OFC)*, 2018, paper W1G.6.

[10] S. T. Le and H. Bülow, "High Performance NFDM Transmission with b-modulation," in *Proc. ITG-Fachbericht 279: Photonische Netze*, Leipzig, Germany, June 2018.

[11] X. Yangzhang, .V. Aref, S. T. Le, H. Bülow, and P. Bayvel, "400 Gbps Dual-polarisation Nonlinear Frequency-division Multiplexed Transmission with b-Modulation," in *Proc. 2018 European Conference on Optical Communication (ECOC)*, Italy, 2018.

[12] T. Gui, G. Zhou, C. Lu, A. P. Lau, and S. Wahls, "Nonlinear frequency division multiplexing with b-modulation: shifting the energy barrier," *Optics Express*, vol. 26, no. 21, pp. 27978–27990, 2018.

[13] X. Yangzhang, V. Aref, S. T. Le, H. Bülow, D. Lavery and P. Bayvel, "Dual-Polarization Non-Linear Frequency-Division Multiplexed Transmission With b-Modulation," *J. Lightwave Technol.*, vol. 37, no. 6, pp. 1570–1578, 2019.

[14] X. Yangzhang, S. T. Le, V. Aref, H. Bülow, D. Lavery and P. Bayvel, "Experimental Demonstration of Dual-Polarization NFDM Transmission With b -Modulation," *IEEE Photon. Technol. Lett.*, vol. 31, no. 11, pp. 885–888, 2019.

[15] T. Aktosun and V. G. Papanicolaou, "Recovery of a potential from the ratio of reflection and transmission coefficients", *J. Math. Phys.*, vol. 44, pp. 4875–4883, 2003.

[16] T. Aktosun, "Inverse scattering on the line with incomplete scattering data", *Contemp. Math.*, vol. 362, 2004.

[17] P. Sacks, "An inverse problem in coupled mode theory", *J. Math. Phys.*, vol. 45, pp. 1699-1710, 2004.

[18] A. Vasylchenkova, J. E. Prilepsky, N. B. Chichkov, and S. K. Turitsyn, "Combining the Discrete NFT Spectrum with b-modulation for High Efficiency Optical Transmission," in *Proc. CLEO/Europe-EQEC*, paper CI-2.5, June 2019, Munich, Germany.

[19] V. Kotlyarov and D. Shepelsky, "Planar unimodular Baker-Akhiezer function for the nonlinear Schrödinger equation," *Ann. Math. Sci. Appl.*, vol. 2, pp. 343–384, 2018.

[20] M. Kamalian, A. Vasylchenkova, D. Shepelsky, J. E. Prilepsky, and S. K. Turitsyn. "Signal Modulation and Processing in Nonlinear Fibre Channels by Employing the RiemannHilbert Problem," *J. Lightwave Technol.*, vol. 36, no. 24, pp. 5714–5727, 2018.

[21] B. Ya. Levin, "Lectures on Entire Functions", *Transl. Mathem. Monographs*, vol. 150, AMS, 1996.

[22] S. Wahls and V. Vaibhav, "Fast inverse nonlinear Fourier transforms for continuous spectra of Zakharov-Shabat type,', arXiv preprint arXiv:1607.01305 (2016).

[23] S. Wahls and V. Vaibhav, "Introducing the fast inverse NFT," in *Proc. Optical Fiber Communications Conference (OFC)*, 2017.

[24] V. Aref, "Control and Detection of Discrete Spectral Amplitudes in Nonlinear Fourier Spectrum," arXiv preprint arXiv:1605.06328 (2016).